INVESTIGATIONS ON THE ANALYSIS AND DESIGN OF APERIODIC FREQUENCY SELECTIVE SURFACES FOR SPACE APPLICATIONS

M. Zhou[1], S. B. Sørensen[1], N. Vesterdal[1], R. Dickie[2], R. Cahill[2], and G. Toso[3]

[1]*TICRA, Copenhagen, Denmark*
[2]*Queen's University of Belfast, Belfast, Northern Ireland, UK*
[3]*ESA ESTEC, Noordwijk, The Netherlands*

ABSTRACT

An investigation on the design of aperiodic FSS is presented. First, an accurate yet efficient method which allows the analysis of finite sized aperiodic FSS has been developed. Subsequently, an optimisation method is implemented which optimises all the FSS elements to obtain an FSS design with an aperiodic element layout. Preliminary designs of aperiodic FSS are presented and the numerical results are discussed.

Key words: Frequency selective surfaces (FSS), aperiodic FSS, optimisation.

1. INTRODUCTION

Frequency selective surfaces (FSS) consist of periodic arrays of passive resonant patch, slot, or aperture elements, which are arranged on planar or curved surfaces [1]. The geometry of the unit cells is selected to obtain the required spectral response for beam splitting, and the structures are usually designed for plane wave illumination at oblique incidence. For space applications, FSS are widely used in various antenna systems, e.g., beam waveguides, quasi-optical (QO) networks, etc. Despite having existed for several decades, a technological problem that still needs to be solved is related to the design of FSS that can be positioned close to the feed system. This is desirable in order to simultaneously reduce the manufacturing cost of the FSS and produce lighter and more compact instruments. In an on-going ESA activity, it is proposed to overcome the limitations imposed on the design of conventional FSS by designing a new type of structure based on the larger number of degrees of freedom obtained by exploiting an aperiodic element layout.

The RF design of conventional FSS is currently done at the unit-cell level where an infinite array consisting of identical unit-cells illuminated by a plane wave is assumed. The unit-cell is then optimised to fulfil a set of reflection and transmission band loss specifications from which the final design is obtained. Several disadvantages are associated with this design approach. First, the finite size of the FSS is not accounted for during the optimisation. Second, the actual distribution of the amplitude, the phase, and the incidence angle of the illuminating field are not taken into account. Third, plane wave illumination is assumed and the near-field properties of the feed are neglected. All these factors combined will result in an FSS design that may have suboptimal performance when positioned close to the feed system. Furthermore, this methodology is not suitable for the design of aperiodic FSS. Full-wave methods on entire FSS do exist, thus accounting for all effects such as mutual coupling, finiteness, actual illuminations etc., but at the expense of high computational complexity, even when acceleration techniques are applied. Consequently, such methods are not suitable for optimisation purposes.

In this work, we present some results related to the analysis and design of aperiodic FSS, which attempt to circumvent the aforementioned issues associated with the current design process. The first step is the development of an accurate yet computationally efficient analysis method that allows the modelling of the entire finite size of the FSS as well as mutual coupling and the actual illumination across the surface of the planar structure. The method will be presented and compared with full-wave simulations on representative antenna system configurations to assess the accuracy of the method. This method is then incorporated in to optimisation routines, which will allow the optimisation of all unit-cell elements to arrive at an FSS design with an aperiodic element layout.

This paper is organised as follows. In Section 2, the analysis method that has been developed is presented. In Section 3, the procedure for the design of aperiodic FSS is described and preliminary results are presented. Conclusions and suggested future work are given in Section 4.

2. HYBRID PMOM/PO METHOD

For the analysis of finite sized aperiodic FSS, a hybrid Periodic Method of Moment (PMoM) and Physical Optics (PO) method has been developed and will be described in this section.

In the PMoM/PO method, each array element is analysed

assuming local periodicity, i.e., the individual element is assumed to be located in an infinite array of identical elements. The reflection/transmission characteristics of each element are determined by a PMoM solver and are subsequently used to form equivalent currents from which the near or far field is calculated. In our case, the PMoM solver uses an integral equations solution based on the spectral domain method of moment (SDMoM), which is applicable to multilayered planar printed structures.

The PMoM/PO has been applied on reflectarrays with good accuracy [2, 3], and is extended to configurations without ground plane.

2.1. Spectral Domain Method of Moments

The SDMoM used in this work is based on the formulation presented in [4] and it can handle an arbitrary number of dielectric layers. In the SDMoM, one can either discretise unknown electric surface currents (patch type FSS) or unknown electric apertures fields (slot type FSS).

To ensure an accurate yet efficient analysis, suitable basis functions must be selected to reduce the number of Floquet harmonics and the total number of basis functions. In our case, the higher-order Legendre basis functions from [5] are used due to their efficiency, accuracy, and flexibility [6].

2.2. Near- and Far-field Calculations

The equivalent currents are constructed on a surface enclosing the entire structure and are defined by

$$J_\mathrm{S} = \hat{n} \times H, \quad M_\mathrm{S} = -\hat{n} \times E, \quad (1)$$

where E and H are the total electric and magnetic fields at the surface and $\hat{n}$ is the outward unit vector normal to that surface, see Figure 1. Since the edge illumination of such structures are usually very low ($< -20\,\mathrm{dB}$), the total field at the edges are assumed to be zero and the equivalent currents are computed only in the top and bottom surface of the structures.

For the calculation of the equivalent currents, the total electric and magnetic fields at the top and bottom surfaces are determined using reflection and transmission coefficients (obtained from the SDMoM). Due to the periodicity, the equivalent currents for each array element are calculated only within its own unit-cell, as illustrated in Figure 2. The equivalent currents for the ith and jth element are shown with solid and dashed lines, respectively. Thus, the contribution from each array element to
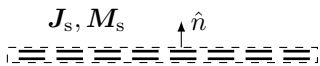
Figure 1. The field equivalence principle for calculating the near- and far-field where equivalent currents are computed on a surface enclosing the entire structure.
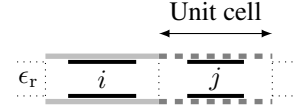
Figure 2. Calculation of the equivalent currents. The equivalent currents for the ith and jth element are shown with solid and dashed lines, respectively.

the equivalent currents is restricted to its unit-cell. The total electric field on the top (E_j^top) and bottom (E_j^bottom) surface of the unit-cell of element j is given by:

$$E_j^\mathrm{top} = (\overline{R}_j + \overline{I})\, E_j^\mathrm{i}, \quad (2a)$$
$$E_j^\mathrm{bottom} = \overline{T}_j\, E_j^\mathrm{i}, \quad (2b)$$

where E_j^i is the incident electric field at element j, $\overline{I}$ is the identity matix, and $\overline{R}_j$ and $\overline{T}_j$ are the reflection and transmission coefficient matrix, respectively, of element j. The total magnetic field can be readily obtained using the plane wave relation.

By repeating this procedure for all array elements, equivalent currents on the surface covering all elements are constructed from which the near- or far-field is determined.

2.3. Representation of the Incident Field

In the PMoM/PO method, each array element is assumed to be illuminated by a locally plane wave. To ensure an accurate solution, the real pattern of the source, obtained by either measurements or an accurate model of the source should be used to compute the polarisation, amplitude, and phase of the incident plane wave on each array element.

The direction of the incident plane wave on each array element is determined by Poynting's vector, thus for element j, the local propagation direction is given by

$$\hat{k}_j^\mathrm{i} = \frac{\mathcal{R}e(E_j^\mathrm{i} \times H_j^{\mathrm{i}*})}{|\mathcal{R}e(E_j^\mathrm{i} \times H_j^{\mathrm{i}*})|}, \quad (3)$$

where H_j^i is the incident magnetic field at element j.

For configurations where the FSS surface is located far away from the source, the assumption of plane wave incidence is accurate. For cases where the surface is located in the near-field region of the source a plane wave expansion (PWE) of the source field is necessary in order to ensure an accurate analysis. The PMoM analysis is then performed for each plane wave and subsequently added to yield the final results. In this approach, the representation of the incident field is exact, but the overall computation becomes very time consuming. To circumvent the calculation of the reflection/transmission coefficients of all array elements for each plane wave, the coefficients can be calculated in advance and stored in a look-up table which

is accessed during the analysis, thereby significantly reducing the computation time. This look-up table can also be used during the optimisation of an aperiodic FSS as will be mentioned in Section 3.2.

2.4. Verification Example

In the following, the PMoM/PO method will be applied to configurations without ground plane to verify its accuracy on such structures. As test case, consider the configurations shown in Figure 3. The distance between the horn aperture and the FSS centre is approximately 335 mm. To facilitate a reference solution, the FSS element used in this case is a simple two layer free-standing square aperture element. The geometry is shown in Figure 4. The length of the square aperture is 4.38 mm, the unit-cell is square with a length of 5 mm, and the separation between the two layers is 5.92 mm. The rim of the FSS is elliptical with major and minor axes of 270 mm and 240 mm, respectively. No dielectrics are used to allow a full-wave solution of the entire structure. The FSS is designed to be transparent at 45° for TM polarisation at 24 GHz. The spectral response is shown in Figure 5. The horn used in the simulations is a theoretical Gaussian beam feed with a diameter of 120 mm.

In Figure 6 the feed pattern with and without the presence of the FSS at 24 GHz is shown. The radiation patterns are calculated using PMoM/PO (cyan) and PMoM/PO where a PWE of the feed is used as illumination (red), and compared to the reference solution obtained using the full-wave MoM with MFLMM (black) in GRASP [7]. The patterns are shown in the feed coordinate system in Figure 3.

It is observed that most of the feed radiation is transmitted through the FSS, however, some reflection is observed around $\theta = 90°$. This reflection is predicted by all three methods, but it is evident that the agreement between MoM and PMoM/PO w/PWE is better than using PMoM/PO without PWE. This is also illustrated in Figure 7 where a close up view of the transmitted feed pattern is shown. It is seen that the PMoM/PO w/PWE is more accurate than the standard PMoM/PO where a locally plane wave for each array element is used. This result is expected since the FSS is located in the near-field
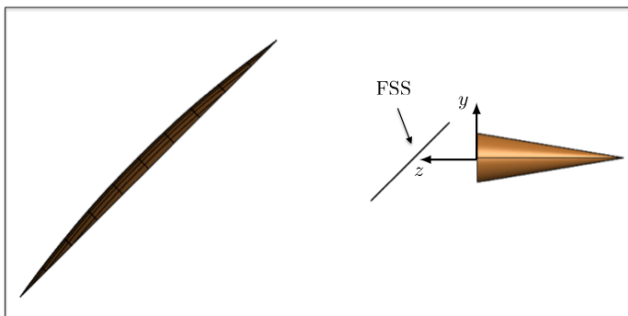
Figure 3. Test configuration.

(a)

(b)
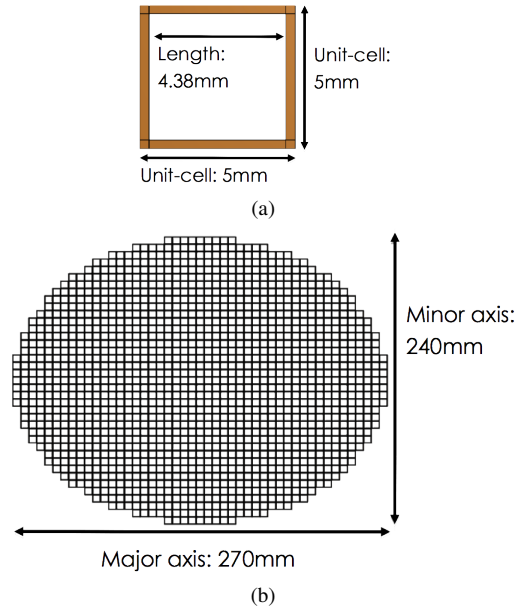
Figure 4. (a) Geometry of two layer free standing square aperture element, (b) the dimensions of the entire FSS.

region of the feed horn. For configurations where the FSS is located further away from the source, the assumption of a locally plane wave for each array element is accurate.

Based on these results, it can be concluded that the accuracy of the PMoM/PO method is very good if the incident field is accurately represented.

3. DESIGN OF APERIODIC FSS

Although the concept of aperiodic FSS bears strong similarity with other types of quasi-periodic surfaces, e.g., transmitarrays/reflectarrays or metasurfaces, the main function of the FSS is different as compared to those structures. In a reflectarray/transmitarray, the purpose of the quasi-periodic surface is to shape/steer the reflected/transmitted beam to obtain a specific desired pattern. This is not the case in an FSS, thus the design approach of an aperiodic FSS is expected to be somewhat different and is to the best of the authors knowledge something new. Nevertheless, as the starting point, we would like to draw on the experience from the design of quasi-periodic surfaces and adapt these for the design of aperiodic FSS.

3.1. Design Methodology

In our approach, the RF design of an aperiodic FSS is done in 2 steps: First, a periodic FSS element is selected and optimised to fulfil certain reflection/transmission characteristics. Second, the aperiodic element layout is obtained by optimising the geometry of all the array elements to fulfil certain optimisation goals while taking
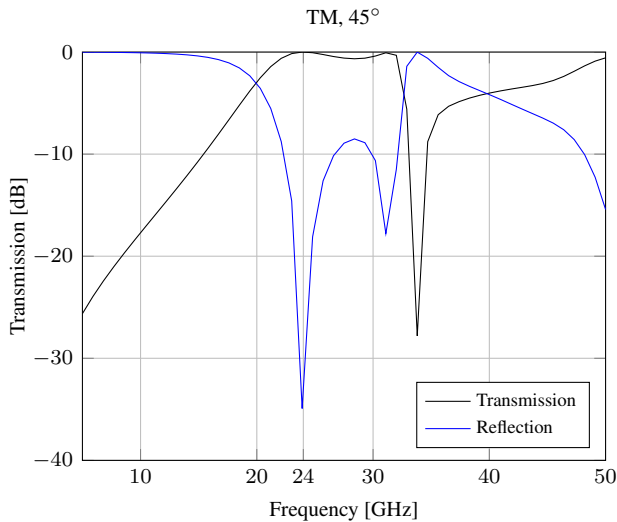
Figure 5. *Spectral response of two layer free standing square aperture FSS element.*
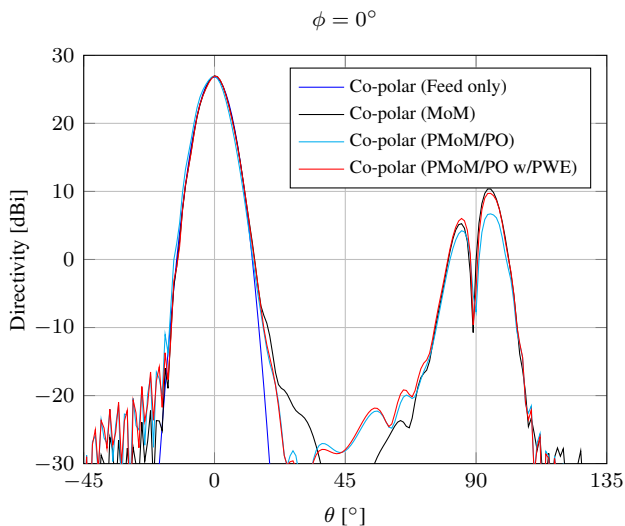
Figure 6. *The feed pattern with and without the presence of the FSS at 24 GHz for TM polarisation with 45° incidence. The radiation patterns are calculated using MoM, PMoM/PO, and PMoM/PO with PWE and are shown in the feed coordinate system in Figure 3.*

into account the finite size of the FSS as well as the mutual coupling and the actual illumination across the surface of the FSS. Several types of optimisation goals have been implemented and tested and are either based on the far-field or the near-field of the FSS.

3.2. Selection/Optimisation of Array Element

Based on the application at hand, a suitable FSS element will be selected. Once an element is determined, an optimisation of the element in a periodic environment is performed from which a number of geometrical parameters,
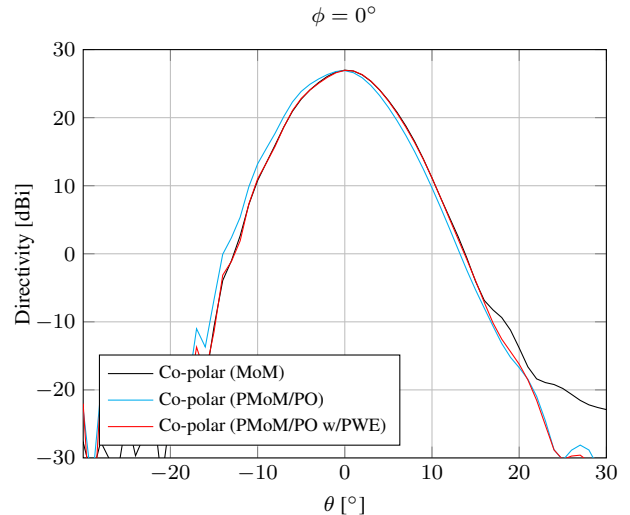
Figure 7. *Zoomed view of the transmitted feed pattern at 24 GHz for TM polarisation with 45° incidence. The radiation patterns are calculated using MoM, PMoM/PO, and PMoM/PO with PWE and are shown in the feed coordinate system in Figure 3.*

which have an impact on the reflection and transmission response of the element are identified. The element response is subsequently fully characterised by sweeping these geometrical parameters, thereby generating a look-up table (this can be the same look-up table as mentioned in Section 2.3) that can be accessed and interpolated during the subsequent optimisation, which will be described in the following sections. In this way, the need to analyse all array elements at each optimisation iteration is avoided.

The time for generating the look-up table can span between minutes to hours depending on the complexity of the element and the number of frequencies etc. However, the look-up table is only generated once and can be reused.

For the aperiodic designs that will be presented later in the paper, we consider an existing element design that was presented in [8]. The FSS geometry is shown in Figure 8a and consists of a two FSS's with linear slot elements separated by a low-permittivity spacer with thickness of 4 mm and relative permittivity $\epsilon_r < 1.03$. The linear slots are $L = 4.7$ mm long and $W = 0.25$ mm wide. The unit-cell is square with a side length of $D = 5.3409$ mm. The FSS is illuminated from the incidence angle $\theta = 45°, \phi = 0°$, where $\phi = 0°$ corresponds to the direction perpendicular to the slots.

The spectral response for TE polarisation is shown in Figure 8b. For simplicity, $\epsilon_r = 1.0$ is used in simulations. It is seen that the FSS is transparent between 30 and 32 GHz.

For this element, the geometrical parameter that will be optimised is the slot length L. A look-up table containing

(a)

TE, 45°

(b)
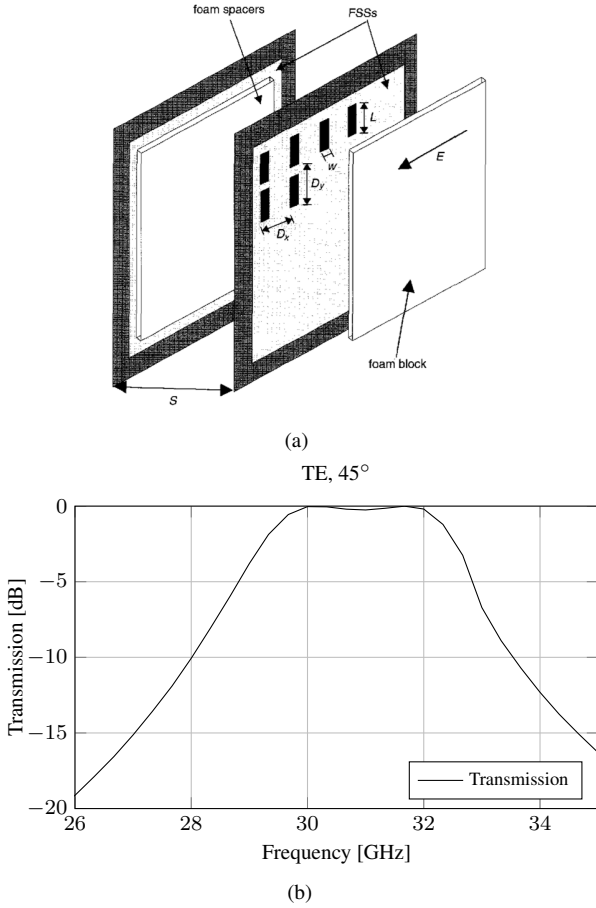
Figure 8. (a) Geometry of the dual-layer FSS from [8], and (b) its spectral response.

the scattering response of the element as function of L is generated and will be used in the subsequent optimisations.

3.3. Far-field Optimisation Approach (FFA)

In a typical application of an FSS, the reflected or transmitted field from the FSS will propagate through a quasi-optical network and end up illuminating a large reflector antenna. It seems reasonable to maximise the efficiency of this reflector antenna and thus to optimise the efficiency of the far-field pattern of the FSS. Such a goal has been implemented and tested.

The directivity of a focused reflector antenna is given by

$$D = \frac{4\pi A}{\lambda^2} \eta_{\text{total}} \qquad (4)$$

where D is the peak directivity, A is the aperture area of the reflector and η_{total} is the total efficiency, which can be split into a number of efficiency factors

$$\eta_{\text{total}} = \eta_{\text{spill-over}} \cdot \eta_{\text{amplitude}} \cdot \eta_{\text{phase}} \cdot \eta_{\text{pol}} \qquad (5)$$

i.e. spill-over efficiency, amplitude efficiency, phase efficiency and polarisation efficiency. The efficiency factors are calculated using the FSS far-field within a conical far-field region corresponding to the opening angle of the reflector antenna. By using an aperiodic element layout, the total efficiency can be maximised, which will maximise the peak directivity of the reflector antenna. But since an FSS with varying patch sizes is also capable of beam shaping it may give undesired side effects. Typically the beam will be shaped such that the amplitude efficiency is improved at the expense of spill over, phase errors and sidelobes, which may not be acceptable in a quasi-optical network. Various modifications of this efficiency goal have been investigated in order to retain the original beam shape, such as a suitable choice of the beam cone angle and removal of the amplitude efficiency factor from the efficiency product. With such modifications the efficiency becomes a useful optimisation goal although an optimum efficiency does not necessarily minimise the reflection of a transmitting FSS or the transmission through a reflecting FSS. Further investigations on this matter are currently on-going.

To shown an example of the use of the far-field optimisation approach, let us again consider the test configuration as shown in Figure 4, where the FSS is elliptical with a major and minor axis of 270 mm and 240 mm, respectively. We then use the far-field optimisation approach to optimise the efficiency of the FSS at 30 GHz. The aperiodic FSS element layout is shown in Figure 9, where the slot length L distribution over the FSS surface is shown. Note that different colors refer to different slot dimensions. Furthermore, it is seen that L spans from 4.70 mm to 4.82 mm, thus the difference in the slot lengths of the elements is small. Nonetheless, it is seen that the element layout follows the illumination pattern of the FSS.

The feed pattern with and without the presence of the aperiodic FSS is shown in Figure 10 and compared to that in

Slot length L distribution over FSS surface [mm]
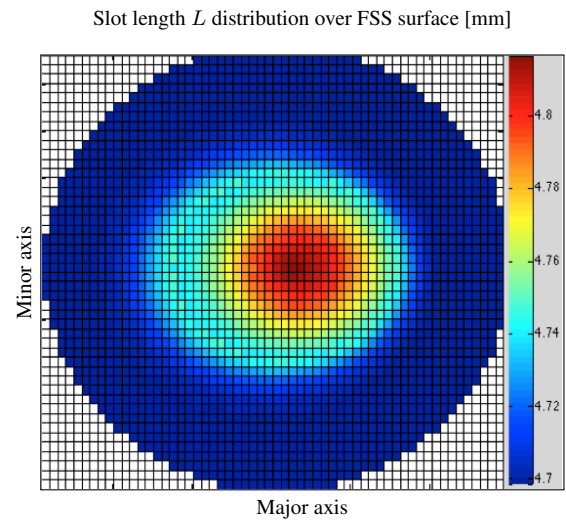
Figure 9. The slot length L distribution over the FSS surface obtained using the far-field optimisation approach.

the presence of the corresponding periodic FSS. Similar to the results shown before, most of the feed radiation is transmitted through the FSS, however with some reflection around 90°.

At 30 GHz, it is observed that the reflected pattern at $\theta = 90°$ is reduced using the aperiodic FSS layout as compared to that of the periodic FSS, without significantly shaping the transmitted beam. However, as expected, this reduction in reflection is obtained at the cost of a degraded performance at 32 GHz since the optimisation was only performed at 30 GHz. It should also be mentioned that the transmitted beam at 30 GHz when using the optimised aperiodic FSS will have a better illumination efficiency on the main reflector as compared to when using the periodic FSS, resulting in higher peak directivity from the main reflector.
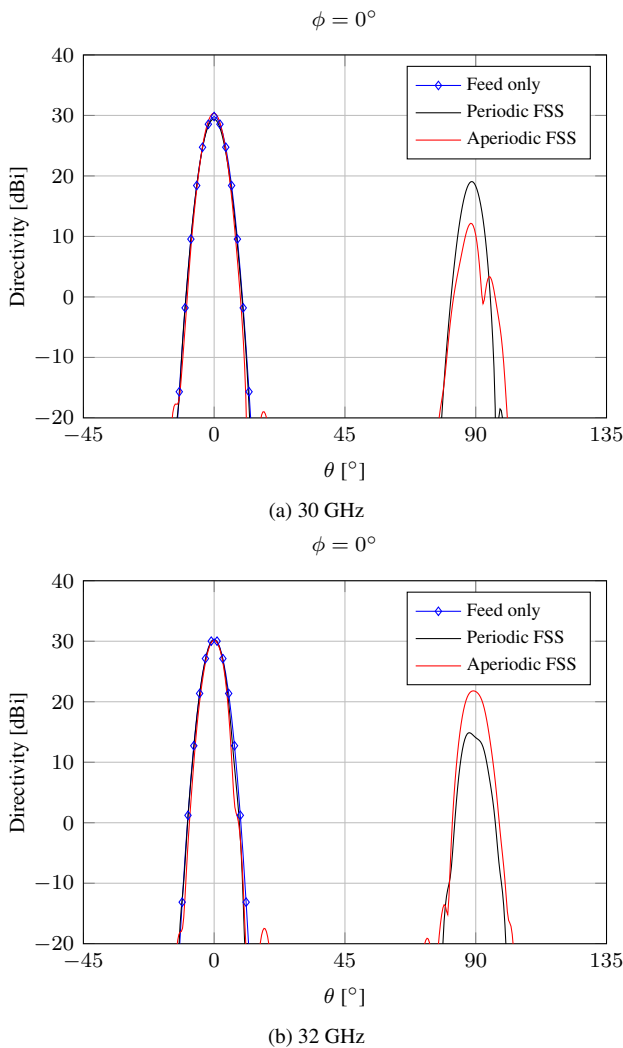
Figure 10. The feed pattern with and without the presence of the FSS at 30 and 32 GHz for TE polarisation. The radiation patterns are calculated using PMoM/PO with PWE and shown in the feed coordinate system in Figure 3.

3.4. Near-field Optimisation Approach (NFA)

Another optimisation approach is to optimise the near-field of the FSS. In this approach, depending on transmission or reflection, the optimisation is performed on the transmitted/reflected field at the back/front surface of the FSS. For the case of transmission which is considered here, the FSS elements are optimised to minimise the reflected near-field of the entire FSS.

An example of an aperiodic FSS obtained using the NFA is shown in Figure 11. This FSS is optimised to minimise the reflected near-field of the FSS at 30 GHz. Similar to before, we consider the test configuration from Figure 3. The feed pattern with and without the presence of the aperiodic FSS is shown in Figure 12 and compared to that in the presence of the aforementioned aperiodic FSS designed using the FFA. It is seen in Figure 12a that the FSS obtained using the NFA gives less reflection compared to that designed using the FFA. However, this is obtained at the cost of increased side lobe levels as well as lower peak directivity. Furthermore, although the reflection has been further reduced, the illumination efficiency of the NFA design on the main reflector will not be as good as that of the FFA design.

Again, the performance at other frequencies degrade since the optimisation is only performed at 30 GHz.

It is worthwhile to note that the element layouts in Figure 9 and Figure 11 are quite different. This is presumably the direct consequence of the different optimisation goals used to arrive at these designs. In addition, the element distribution in Figure 11 is not as smooth as in Figure 9 which is a result of a limitation that is currently in the NFA implementation, which can be easily solved.

Based on the results presented here, aperiodic FSS may
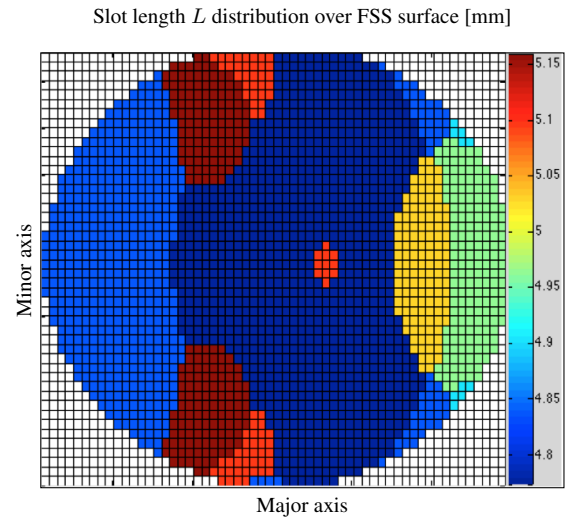
Figure 11. The slot length L distribution over the FSS surface obtained using the near-field optimisation approach.

(a) 30 GHz
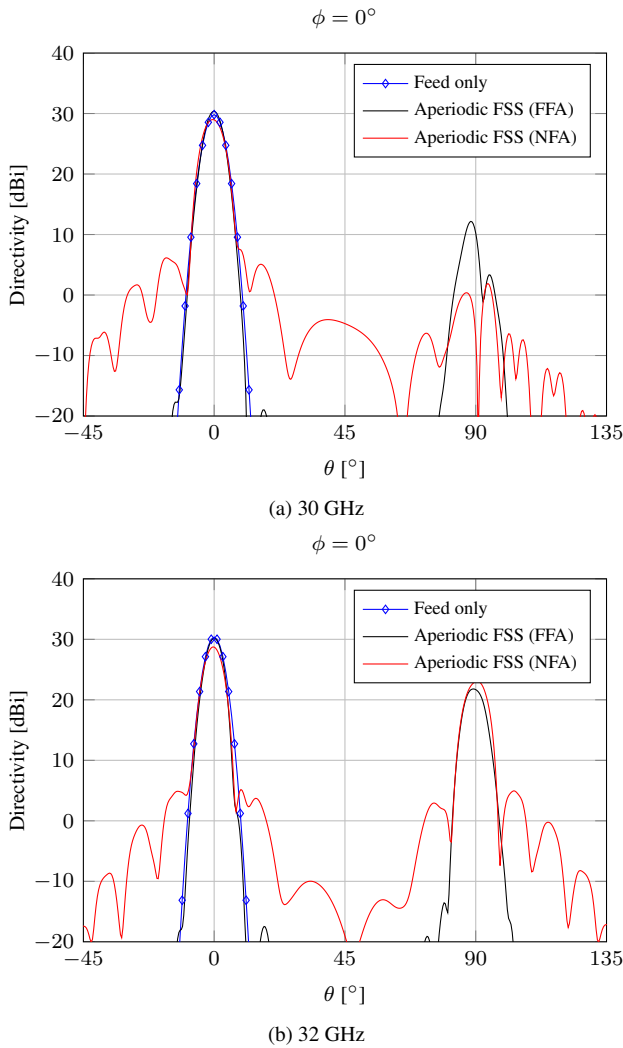
(b) 32 GHz

Figure 12. The feed pattern with and without the presence of the FSS at 30 and 32 GHz for TE polarisation. The radiation patterns are calculated using PMoM/PO with PWE and shown in the feed coordinate system in Figure 3.

be useful, but to fully understand the potential of the increased degree of freedom of an aperiodic FSS, further investigations are needed.

4. CONCLUSIONS AND FUTURE WORK

It has been shown that a standard quasiperiodic FSS may not be the optimum design for an FSS located within the near field of a feed. The near-field effects of the feed can, however, be efficiently compensated for by using an aperiodic FSS which increases the available number of degrees of freedom in the design. However, this means that the design process becomes significantly more complicated since the FSS is capable of changing the shape of the beam, e.g., focus or defocus the beam. This may however be useful, for some applications, to obtain a certain desired beam shape. Optimisation goals must be chosen carefully to obtain the desired performance of the FSS. Further work is needed in a number of areas:

- Identification of desired beam characteristics in terms of, e.g., beam shape, Gaussicity, and efficiency.

- Definition of new optimisation goals for obtaining the desired beam and efficiency, e.g., combinations of near- and far-field optimisation specifications.

- Advanced design of the FSS unit-cell with additional degrees of freedom.

- Optimisation at multiple frequencies for bandwidth improvement.

REFERENCES

[1] T. K. Wu, *Frequency Selective Surface and Grid Array*. Wiley Interscience, 1995.

[2] M. Zhou, S. B. Sørensen, O. S. Kim, E. Jørgensen, P. Meincke, and O. Breinbjerg, "Direct optimization of printed reflectarrays for contoured beam satellite antenna applications," *IEEE Trans. Antennas Propag.*, vol. 61, no. 4, pp. 1995–2004, 2013.

[3] M. Zhou, S. B. Sørensen, O. S. Kim, E. Jørgensen, P. Meincke, O. Breinbjerg, and G. Toso, "The generalized direct optimization technique for printed reflectarrays," *IEEE Trans. Antennas Propag.*, vol. 62, no. 4, pp. 1690–1700, 2014.

[4] G. Kristensson, S. Poulsen, and S. Rikte, "Propagators and scattering of electromagnetic waves in planar bianisotropic slabs - an application to frequency selective structures," *Progr. Electromagn. Res. (PIER)*, vol. 48, pp. 1–25, 2004.

[5] E. Jørgensen, J. Volakis, P. Meincke, and O. Breinbjerg, "Higher order hierarchical Legendre basis functions for electromagnetic modeling," *IEEE Trans. Antennas Propag.*, vol. 52, no. 11, pp. 2985 – 2995, 2004.

[6] M. Zhou, E. Jørgensen, O. S. Kim, S. B. Sørensen, P. Meincke, and O. Breinbjerg, "Accurate and efficient analysis of printed reflectarrays with arbitrary elements using higher-order hierarchical Legendre basis functions," *IEEE Antennas Wireless Propag. Lett.*, vol. 11, pp. 814–817, 2012.

[7] "GRASP Software," TICRA, Copenhagen, Denmark.

[8] R. Cahill, J. C. Vardaxoglou, and M. Jayawardene, "Two-Layer mm-Wave FSS of Linear Slots Elements with Low Insertion Loss," *IEE Proc. Microw. Antennas Propag.*, vol. 148, no. 6, pp. 410–412, 2001.